Geophysical Research Letters

RESEARCH LETTER
10.1029/2024GL109874

On the Westward Shift and Strengthening of the Atmosphere-To-Ocean Bjerknes Feedback in the Tropical Pacific Since 2000

Zongrong Li[1,2,3], Ruiqiang Ding[1], Jiangyu Mao[2], Zhengyi Ren[2,3], and Jianping Li[4,5]

[1]State Key Laboratory of Earth Surface Processes and Resource Ecology, Beijing Normal University, Beijing, China, [2]State Key Laboratory of Numerical Modeling for Atmospheric Sciences and Geophysical Fluid Dynamics (LASG), Institute of Atmospheric Physics, Chinese Academy of Sciences, Beijing, China, [3]College of Earth Science, University of Chinese Academy of Sciences, Beijing, China, [4]Key Laboratory of Physical Oceanography-Institute for Advanced Ocean Studies, Qingdao National Laboratory for Marine Science and Technology, Ocean University of China, Qingdao, China, [5]Laoshan Laboratory, Qingdao, China

Abstract The behavior of the El Niño–Southern Oscillation (ENSO) has undergone significant changes since the year 2000. Meanwhile, a notable westward shift and strengthening in the atmosphere-to-ocean Bjerknes feedback were observed. We find that this shift can be primarily attributed to a weakened relationship between the zonal gradient of precipitation anomaly and that of sea surface temperature (SST) anomaly since 2000.This weakened relationship is a comprehensive manifestation of reduced El Niño-related precipitation anomalies in the central-eastern tropical Pacific and increased anomalies in the western tropical Pacific. These changes are connected to the mean state change in the tropical Pacific after 2000, where the cooler background SSTs in the central-eastern tropical Pacific suppress upward motion, and the warmer background SSTs in the western tropical Pacific promote upward motion in the overlying atmosphere. Our findings offer a potential explanation for the westward shift and strengthening in the atmosphere-to-ocean Bjerknes feedback since 2000.

Plain Language Summary The El Niño–Southern Oscillation (ENSO) is a climate phenomenon that plays a major role in global weather and climate systems. The development of ENSO is mainly attributed to a positive feedback known as the Bjerknes feedback, which represents the atmospheric response to the oceanic forcing and vice versa. It is noted that ENSO has behaved differently since the year 2000. Concurrently, a pronounced westward movement and strengthening in the atmosphere-to-ocean Bjerknes feedback have also been observed. Analyses show that changes in the Bjerknes positive feedback are largely due to a weakened relationship between anomalous rainfall patterns and sea surface temperatures (SSTs). This implies that during El Niño events, there is less rainfall in the central and eastern parts of the tropical Pacific, and more rainfall in the western tropical Pacific. These changes are linked to a cooling of background SSTs in the central-eastern tropical Pacific, which reduces the upward air movement and rainfall in that region, and a warming of background SSTs in the western Pacific, which promotes the upward air movement and rainfall.

Key Points:

- Westward shift and strengthening of the atmosphere-to-ocean Bjerknes feedback in the tropical Pacific have been observed since 2000
- A weakened precipitation-to-sea surface temperature (SST) response drives the changes in the atmosphere-to-ocean Bjerknes feedback
- Changes in precipitation-to-SST response are linked to the interdecadal shift in the tropical Pacific background state

Supporting Information:

Supporting Information may be found in the online version of this article.

Correspondence to:

R. Ding,
drq@bnu.edu.cn

Citation:

Li, Z., Ding, R., Mao, J., Ren, Z., & Li, J. (2024). On the westward shift and strengthening of the atmosphere-to-ocean Bjerknes feedback in the tropical Pacific since 2000. *Geophysical Research Letters*, *51*, e2024GL109874. https://doi.org/10.1029/2024GL109874

Received 18 APR 2024
Accepted 10 JUN 2024

Author Contributions:

Conceptualization: Zongrong Li, Ruiqiang Ding
Data curation: Zongrong Li, Ruiqiang Ding, Zhengyi Ren
Formal analysis: Zongrong Li, Ruiqiang Ding
Funding acquisition: Ruiqiang Ding, Jiangyu Mao
Investigation: Zongrong Li, Ruiqiang Ding
Methodology: Zongrong Li, Ruiqiang Ding, Jianping Li
Project administration: Ruiqiang Ding
Software: Zongrong Li, Ruiqiang Ding
Supervision: Ruiqiang Ding, Jiangyu Mao, Jianping Li

1. Introduction

The El Niño–Southern Oscillation (ENSO), which is the dominant mode of variability in the coupled ocean-atmosphere system in the tropical Pacific, has wide-ranging effects on the global climate and ecosystems (e.g., Alexander et al., 2002; Larkin & Harrison, 2005; Liu & Alexander, 2007; Plisnier et al., 2000). In the past few decades, there has been extensive research on the theory for the ENSO phenomenon (e.g., Bjerknes, 1969; Cane, 1992; Cane & Zebiak, 1985; Jin, 1997a, 1997b; Timmermann et al., 2018). Bjerknes (1969) first proposed that the development of ENSO events depends on a positive feedback loop between the equatorial ocean and the overlying atmosphere, which is known as Bjerknes positive feedback. The positive feedback loop can be initiated by a positive (negative) sea surface temperature (SST) anomaly in the eastern equatorial Pacific. This positive (negative) SST anomaly diminishes (enhances) the background SST gradient, resulting in weakened (strengthened) trade winds over the equatorial Pacific, which in turn reinforces the initial SST anomaly.

Recent studies have noted that the Bjerknes positive feedback exhibits variations on interdecadal timescales (e.g., Lübbecke & Mcphaden, 2014; Xiang et al., 2013; Zheng et al., 2016). Hu et al. (2017) reported a westward displacement and intensification of the atmosphere-to-ocean Bjerknes feedback in the tropical Pacific since 2000.

Validation: Zongrong Li, Ruiqiang Ding, Jiangyu Mao, Zhengyi Ren
Visualization: Zongrong Li, Ruiqiang Ding
Writing – original draft: Zongrong Li, Ruiqiang Ding

This shift has been thought to be one of the reasons for the reduction in ENSO variability and the shortening of the ENSO cycle, as well as the breakdown of the relationship between warm water volume and ENSO SST anomalies after 2000 (e.g., Bunge & Clarke, 2014; Horii et al., 2012; Hu et al., 2013, 2017; McPhaden, 2012). These changes have sparked considerable interests within the scientific community, as they not only alter the characteristics of ENSO events but also present challenge to the ENSO prediction (Barnston et al., 2012; Kumar et al., 2015; Wang et al., 2010; Xue et al., 2013). However, the underlying mechanisms responsible for the recent changes in the atmosphere-to-ocean Bjerknes feedback after 2000 remain unclear.

In the present study, we utilize a combination of observational data and model simulations to perform a quantitative comparison of the atmospheric subprocesses involved in the Bjerknes feedback, before and after the year 2000. Our results show that the westward shift and strengthening of the atmosphere-to-ocean Bjerknes feedback post-2000 is primarily caused by a weakened response of the zonal precipitation anomaly gradient to the SST anomaly gradient. Through this research, we provide a potential insight into the complex interactions that drive recent changes in the atmosphere-to-ocean Bjerknes feedback, highlighting the critical role of interdecadal shift in the tropical Pacific background state.

2. Data Sets and Methods

2.1. Data Sets

In our observational analyses, the monthly mean SST data used is from the Hadley Centre global sea ice and sea surface temperature (HadISST; Rayner et al., 2003), with a horizontal resolution of 1° × 1°. For monthly mean atmospheric fields, we utilize sea level pressure (SLP), vertical velocity (Omega) and surface momentum flux data from the National Centers for Environmental Prediction–National Center for Atmospheric Research (NCEP–NCAR) reanalysis (Kalnay et al., 1996), as well as precipitation data from the Climate Prediction Center Merged Analysis of Precipitation (CMAP; Xie & Arkin, 1997). The SLP, vertical velocity and precipitation have a horizontal resolution of 2.5° × 2.5°, while the surface momentum flux is on a Gaussian grid. Due to random observational errors and systematic errors, the gridded data sets may exhibit significant uncertainties (Kennedy, 2014). The uncertainties in HadISST data are relatively large in the late 19th and early 20th centuries due to sparse observations and diverse measurement methods (Rayner et al., 2003). The uncertainties in CMAP data primarily arise from insufficient observational coverage and biases in the merging process, especially around 1979 (Xie & Arkin, 1997). The NCEP reanalysis data uncertainties stem from changes in the observing systems and the limited availability of early data, particularly before 1957 (Kalnay et al., 1996). In this study, all the observational and reanalysis data are for the period 1979–2021.

For Atmospheric Model Intercomparison Project (AMIP) simulations, we use outputs of 33 climate models participating in the Coupled Model Intercomparison Project Phase 6 (CMIP6; Eyring et al., 2016) for the period 1979–2014. Due to the varying grid spacings and simulation lengths of different models, all the model outputs are bilinearly interpolated to a 2.5° × 2.5° grid. Details about the models used in this study are summarized in Table S1 of Supporting Information S1. In this paper, the monthly anomalies of observed and simulated data are derived by removing the long-term trend and climatological monthly means from each calendar month. The long-term trend is calculated by fitting a linear regression model of each variable against time. For the observational data, the long-term trend and climatological monthly means are calculated over the period 1979–2021, while for the simulated data, they are calculated over the period 1979–2014.

2.2. Methods

Linear regression technique is utilized to examine the relationships between two different variables. The strength of atmosphere-to-ocean Bjerknes feedback is quantified by the regression of zonal wind stress (τ_x) onto the zonal gradient of SST ($dSST/dx$) (Hu et al., 2017, 2020; Li et al., 2019; Zheng et al., 2014). The zonal gradients in this study are defined as the differences between the area-averaged anomalies over the regions in the eastern tropical Pacific (140°–110°W, 5°S–5°N) and western tropical Pacific (130°−160°E, 5°S–5°N). In these regions, the most significant changes in mean SST anomalies have been observed since the year 2000 (see Figure S1 in Supporting Information S1).

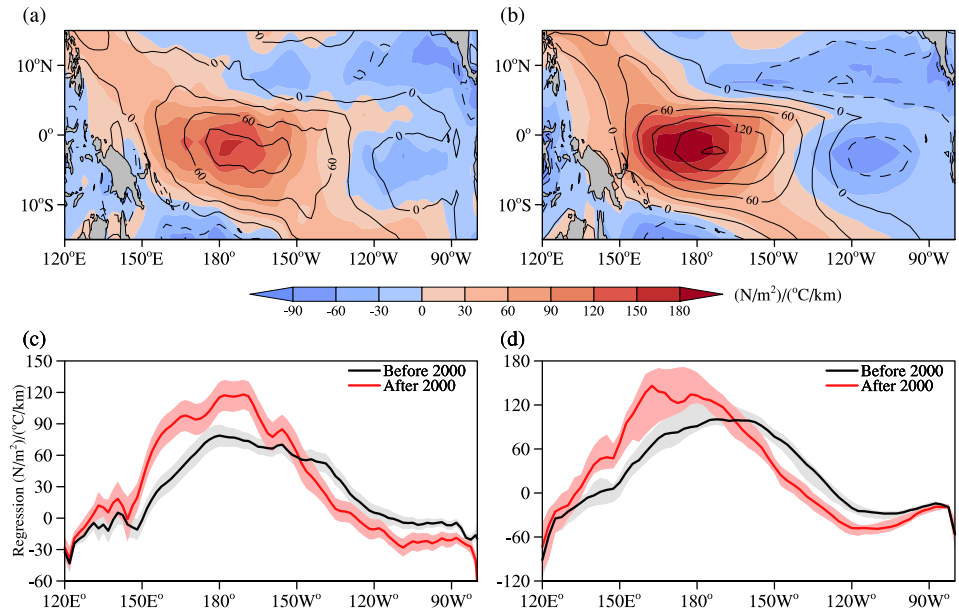

Figure 1. (a) Regression pattern of anomalous zonal wind stress onto the zonal gradient of sea surface temperature (SST) in observations, which denotes the strength of the so-called atmosphere-to-ocean Bjerknes feedback. Contours and shadings represent the periods of 1979–1999 and 2000–2021, respectively. The unit is $(N/m^2)/(°C/km)$ and the contour interval is 30. (b) As in panel (a) but for results in the Atmospheric Model Intercomparison Project (AMIP) multi-model ensemble (MME). Contours and shadings are for the periods of 1979–1999 and 2000–2014, respectively. (c) Regression of anomalous zonal wind stress onto the zonal gradient of SST, averaged between 5°S and 5°N, along with the corresponding error bars (shaded, 95% confidence for a Student's *t* test). Black and red lines represent periods of 1979–1999 and 2000–2021, respectively. (d) As in panel (c), but for the AMIP MME, with black and red lines representing 1979–1999 and 2000–2014, respectively. Pink and gray shadings indicate the interquartile range of regression coefficients in the AMIP simulations, corresponding to the two periods.

3. Results

Figure 1a illustrates the spatial distributions of the atmosphere-to-ocean Bjerknes feedback in the tropical Pacific before and after the year 2000. As can be seen, differences in the strength and position of the atmosphere-to-ocean Bjerknes feedback between two periods are evident. Specifically, during 1979–1999, strong positive feedback is mainly situated in the central–eastern tropical Pacific, with its largest amplitudes located south of the equator between 180° and 150°W (contours, Figure 1a). Compared to 1979–1999, the atmosphere-to-ocean Bjerknes feedback after 2000 exhibits a westward shift, with a significant enhancement in the western equatorial Pacific and northwestern Pacific, as well as a reduction in the central–eastern equatorial Pacific (shadings, Figure 1a). These changes are further evidenced by the zonal distribution of the atmosphere-to-ocean Bjerknes feedback within the equatorial Pacific (5°S–5°N) (Figure 1c), confirming the substantial westward shift of air-sea coupling in the tropical Pacific after 2000 (Bunge & Clarke, 2014; Hu et al., 2017, 2020; Li et al., 2019).

To investigate the key factor potentially driving the westward shift of the atmosphere-to-ocean Bjerknes feedback since 2000, we employed the approach used by Zheng et al. (2014). This approach enables us to examine the changes in the atmospheric subprocesses associated with the Bjerknes positive feedback, as identified by Bjerknes (1969) and further elaborated by Lin (2007):

$$\frac{dSST}{dx} \xrightarrow{\text{Subprocess1}} \frac{dQ}{dx} \approx \frac{dPrecip}{dx} \xrightarrow{\text{Subprocess2}} \frac{dSLP}{dx} \xrightarrow{\text{Subprocess3}} \tau_x$$

These subprocesses include the response of zonal gradient in diabatic heating (Q) to the zonal gradient of SST ($dSST/dx \rightarrow dQ/dx$; Subprocess1), the response of zonal gradient in SLP to the zonal gradient of diabatic heating ($dQ/dx \rightarrow dSLP/dx$; Subprocess2), the impact of the SLP gradient on the zonal wind stress ($dSLP/dx \rightarrow \tau_x$; Subprocess3) (Zheng et al., 2014, 2016). As pointed out by Zheng et al. (2014), diabatic heating is commonly approximated by latent heating associated with precipitation ($Q \approx Precip$), based on the assumption that the

10.1029/2024GL109874

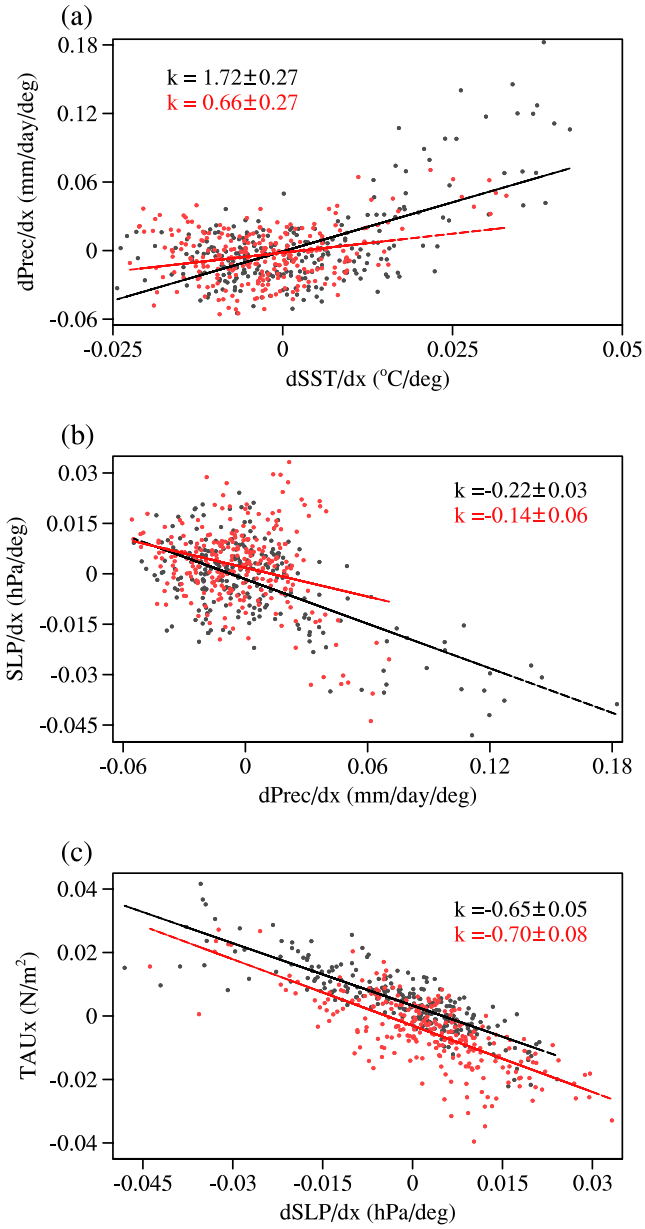

Figure 2. Scatter plots for the (a) zonal gradients of sea surface temperature and precipitation, (b) zonal gradients of precipitation and sea level pressure (SLP), and (c) zonal SLP gradients and area-averaged zonal wind stress anomalies during the period of 1979–1999 (black) and 2000–2021 (red). The solid lines represent the least squares best fit lines, with their slope values and 95% confidence intervals for a Student's *t* test indicated next to them.

contribution from cloud radiative heating is negligible (Lin, 2007). Therefore, in subsequent analyses, the zonal gradient in diabatic heating anomaly is approximated by the corresponding gradient in precipitation anomaly ($dQ/dx \approx dPrecip/dx$). It should be noted that the methodology used here primarily focuses on the changes in *dPrecip/dx* driven by changes in *dSST/dx*, the changes in *dSLP/dx* caused by changes in *dPrecip/dx*, and the changes in τ_x resulting from changes in *dSLP/dx*, while other processes have not been considered.

First, we contrasted the Subprocess1 (*dSST/dx* → *dPrecip/dx*) of the atmosphere-to-ocean Bjerknes feedback between the periods before and after the year 2000. As illustrated in Figure 2a, the sensitivities of zonal gradients of precipitation to zonal gradients of SST exhibit significantly disparities between two periods. Specifically, during the period of 1979–1999, the slope is measured at 1.72 ± 0.27 (mm/day/°C), while for 2000–2021, it reduces to 0.66 ± 0.27 (mm/day/°C). This change indicates that a given value of zonal SST gradient during the period of 2000–2021 can lead to a smaller precipitation gradient compared to that during 1979–1999. We then investigated the changes in two other subprocesses within the atmosphere-to-ocean Bjerknes feedback after the year 2000. The Subprocess2 (*dPrecip/dx* → *dSLP/dx*) of the atmosphere-to-ocean Bjerknes feedback experiences a slight change after 2000, but this change is not statistically significant, with the slopes of the two periods showing no significant difference at a 95% confidence level (Figure 2b). Lastly, the relationship between the zonal gradient of SLP and the area-averaged (160°E−140°W, 5°S–5°N) zonal wind stress anomalies (Subprocess3) also remains relatively stable across both periods (Figure 2c), with a slope of −0.65 ± 0.05 (N/m^2)/(hPa/deg) for 1979–1999 and a slope of −0.70 ± 0.08 (N/m^2)/(hPa/deg) for 2000–2021, respectively. Given the negligible differences in the latter two components between two periods, the westward shift and strengthening of the atmosphere-to-ocean Bjerknes feedback since 2000 can primarily be attributed to the reduced sensitivity of the precipitation heating gradient to the anomalous SST associated with El Niño events.

The spatial patterns of precipitation and vertical velocity (Omega) anomalies associated with El Niño for the two periods offer a potential insight into the weakened response of the precipitation gradient to the SST gradient. Negative values of Omega anomalies signify upward vertical movement of the atmosphere and correspond to positive precipitation anomalies during the El Niño events (Huang & Xie, 2015). Figure 3a shows that the centers of anomalous vertical velocity at 500-hPa pressure level are mainly situated in the central tropical Pacific in both periods. However, notable differences are evident in the strength and location of maximum values between the two periods, as illustrated in Figures 3a and 3b. From 1979 to 1999, the maximum values of vertical velocity anomalies, ranging between −0.018 and −0.024 (hPa/s), are centered at approximately 150°W (contours, Figure 3a). In contrast, during the period of 2000–2021, strong vertical velocity anomalies reach as low as −0.024 (hPa/s) with a westward shift to around 180° (shadings, Figure 3a). This shift is likely to stem from the interdecadal shift in the background conditions of the tropical Pacific (Hu et al., 2013), which represents an aspect of westward shift in tropical Pacific climate variability since 2000 (Li et al., 2019). Specifically, the cooler SST background in the central–eastern tropical Pacific since 2000 suppresses the upward movement and precipitation in the overlying atmosphere induced by the warm SST anomalies associated with El Niño. On the other hand, a warmer warm pool since 2000 promotes stronger upward motion and precipitation in the western tropical Pacific compared to previous years (shadings, Figure 3b). Consequently, the weakening in the response of zonal precipitation gradient to zonal SST

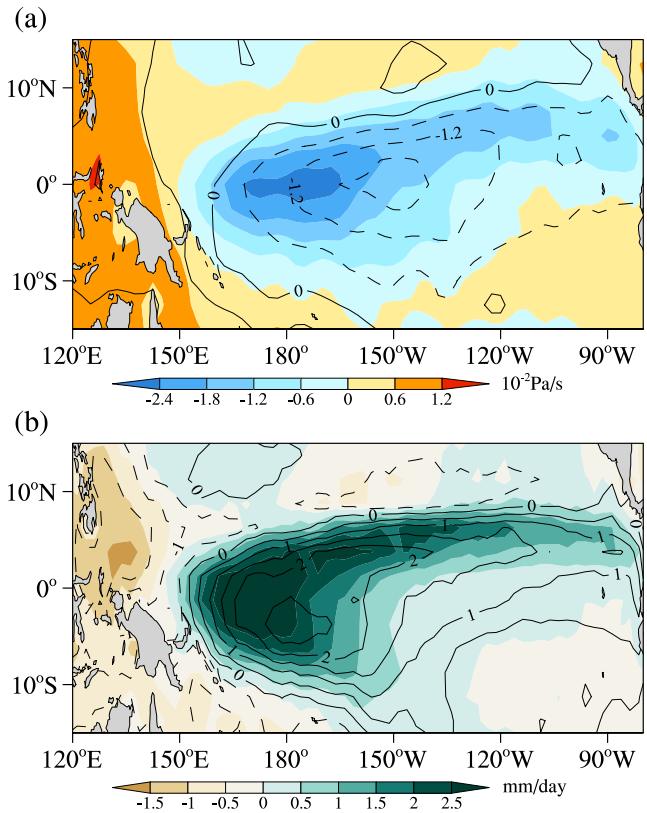

Figure 3. Regression patterns of anomalous (a) Omega at 500-hPa pressure, (b) precipitation and onto the normalized zonal gradient of sea surface temperature. Contours and shadings are for the periods of 1979–1999 and 2000–2021, respectively. The units are 10^{-2} Pa/s and mm/day for anomalous Omega and precipitation, and the corresponding contour intervals are 0.6 and 0.5, respectively.

gradient is actually a comprehensive reflection of the decrease in precipitation anomalies in the central–eastern tropical Pacific as well as the increase in precipitation anomalies in the western tropical Pacific (Figure 2a).

Furthermore, we employed the AMIP simulations to validate the influence of SST background changes on the westward shift of the atmosphere-to-ocean Bjerkens feedback in the tropical Pacific. The phenomenon of the westward shift and strengthening of the atmosphere-to-ocean Bjerknes feedback since 2000 can be well captured by all 33 AMIP runs (see Figure S2 in Supporting Information S1) and the multi-model ensemble (MME) (Figure 1b). The zonal structure of the strength of the atmosphere-to-ocean Bjerknes feedback in the AMIP runs experiences similar changes to the observation after 2000 (lines in Figure 1d), with an increase of approximately 40 (N/m^2)/(°C/km) in the MME of AMIP runs. However, there is a more westward shift of the zonal position of the strongest feedback strength after 2000 in simulations compared to the observations (red line in Figure 1c). This difference may be due to the AMIP simulations running only until 2014, thereby excluding the strong eastern Pacific El Niño event of 2015–2016.

Given that the westward shift and strengthening of the atmosphere-to-ocean Bjerknes feedback since 2000 can be well replicated in the AMIP simulations, we proceeded to examine the influence of changes in the SST background state on the response of the zonal precipitation gradient to the SST gradient based on the AMIP simulations. Under the imposed SST boundary conditions during 1979–2014, nearly all (32 out of 33) of the AMIP simulations exhibit atmospheric changes similar to those in observation since 2000. These changes are characterized by reduced anomalous upward motion and precipitation in the eastern portion of the tropical Pacific, as well as increased upward motion and precipitation anomalies in the central–western portion (see Figures 4a and 4b for the MME and Figures S3–S4 in Supporting Information S1 for each individual model). These changes are linked with a weakened response of the zonal precipitation gradient to the SST gradient in the Subprocess1 of the atmosphere-to-ocean Bjerknes feedback (Figure 4c), confirming that the interdecadal shift in the tropical Pacific background state is the primary driver behind the westward shift and strengthening of the atmosphere-to-ocean Bjerknes feedback since 2000.

4. Summary and Discussion

This study focuses on the profound changes observed in the atmosphere-to-ocean Bjerknes feedback within the tropical Pacific since the year 2000. By investigating three atmospheric subprocesses within the Bjerknes feedback, our findings show that a weaker response of the zonal precipitation gradient to the zonal SST gradient is a major contributor to the westward shift and strengthening of the atmosphere-to-ocean Bjerknes feedback since 2000. This weakened relationship is a comprehensive reflection of decreased precipitation anomalies induced by El Niño-related SST anomalies in the central–eastern tropical Pacific and increased precipitation anomalies in the western tropical Pacific. Further analysis confirms that such changes in the context of ENSO result from the mean state change in the tropical Pacific, where the cooler background SSTs in the central–eastern equatorial Pacific are unfavorable for upward motion and precipitation in the overlaying atmosphere. Conversely, in the western equatorial Pacific, the warmer background SSTs promote enhanced upward motion and precipitation. Different from the research by Zheng et al. (2016), which focused on the overall changes in the strength of the atmosphere-to-ocean Bjerknes positive feedback across the equatorial Pacific, the present study focuses more on the synchronous changes in the position and intensity of the atmosphere-to-ocean Bjerknes positive feedback since 2000. Consequently, the mechanism proposed here provides a distinct perspective on the connection between the interdecadal shift in the atmosphere-to-ocean Bjerknes feedback and the tropical Pacific background state.

The present study primarily focuses on the atmospheric subprocesses in the Bjerknes positive feedback, which is characterized by the atmospheric response to the tropical oceans. Meanwhile, as documented in previous studies,

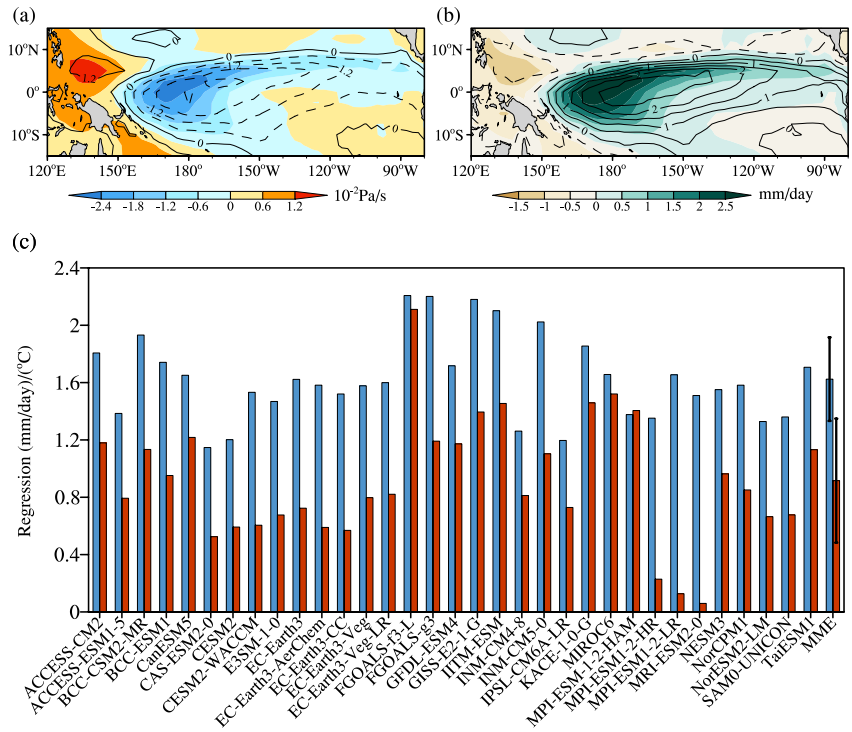

Figure 4. Regression patterns of anomalous (a) Omega at 500-hPa pressure, (b) precipitation and onto the normalized zonal gradient of sea surface temperature (SST) in the Atmospheric Model Intercomparison Project (AMIP) multi-model ensemble (MME). Contours and shadings are for the periods of 1979–1999 and 2000–2014, respectively. The units are 10^{-2} Pa/s and mm/day for anomalous Omega and precipitation, and the corresponding contour intervals are 0.6 and 0.5, respectively. (c) Regression coefficients of the zonal precipitation gradients onto the SST gradients in the AMIP simulations during 1979–1999 (blue) and 2000–2014 (red). The last two bars denote the AMIP MME. The unit is mm/day/°C. The error bars in the MME denote one standard deviation of the regression coefficients from all models.

the changes in oceanic response to wind stress anomalies since 2000 are also significant. For example, Lübbecke and Mcphaden (2014) noted that the weakening of the thermocline feedback after 2000 can be attributed to the reduced response of the thermocline slope to the zonal anomalous wind stress along the equator. However, as pointed out by Wittenberg (2009), historical records can be substantially influenced by sampling variability. Thus, a relatively short observational record may not fully capture the natural characteristics of ENSO. While our findings suggest significant changes in ENSO behavior over recent decades, it is important to consider that some of these observed changes may be influenced by sampling variability rather than solely reflecting changes in the underlying dynamics in the tropics (Martinez-Villalobos et al., 2019). Moreover, an increasing number of studies are recognizing the significant impact of extratropical climate variability on ENSO-related variability in the tropics (e.g., Amaya, 2019; Chang et al., 2007; Ding et al., 2014, 2017, 2022; Fan et al., 2021; Min et al., 2017; Vimont, Battisti, & Hirst, 2003; Vimont, Wallace, & Battisti, 2003; Yu & Kim, 2011; Yu et al., 2010). However, a comprehensive understanding of their influence on the Bjerknes positive feedback remains elusive, highlighting the need for further investigation in this area.

Conflict of Interest

The authors declare no conflicts of interest relevant to this study.

Data Availability Statement

The SST data is available at https://www.metoffice.gov.uk/hadobs/hadisst/ (Rayner et al., 2003). The monthly mean atmospheric fields from NCEP-NCAR Reanalysis can be download at https://psl.noaa.gov/data/gridded/data.ncep.reanalysis.html (Kalnay et al., 1996). The CMAP precipitation data is available at https://psl.noaa.gov/

data/gridded/data.cmap.html (Xie & Arkin, 1997). The CMIP6 data is available at https://aims2.llnl.gov/search/?project=CMIP6/ (Eyring et al., 2016).

Acknowledgments
This work was jointly supported by the National Natural Science Foundation of China (Grant 42225501) and by the Strategic Priority Research Program of the Chinese Academy of Sciences (XDB40000000).

References

Alexander, M. A., Bladé, I., Newman, M., Lanzante, J. R., Lau, N. C., & Scott, J. D. (2002). The atmospheric bridge: The influence of ENSO teleconnections on air-sea interaction over the global oceans. *Journal of Climate*, *15*(16), 2205–2231. https://doi.org/10.1175/1520-0442(2002)015<2205:TABTIO>2.0.CO;2

Amaya, D. J. (2019). The Pacific meridional mode and ENSO: A review. *Current Climate Change Reports*, *5*(4), 296–307. https://doi.org/10.1007/s40641-019-00142-x

Barnston, A. G., Tippett, M. K., L'Heureux, M. L., Li, S., & DeWitt, D. G. (2012). Skill of real-time seasonal ENSO model predictions during 2002–11: Is our capability increasing? *Bulletin of the American Meteorological Society*, *93*(5), 631–651. https://doi.org/10.1175/BAMS-D-11-00111.1

Bjerknes, J. (1969). Atmospheric teleconnections from the equatorial Pacific. *Monthly Weather Review*, *97*(3), 163–172. https://doi.org/10.1175/1520-0493(1969)097%3C0163:ATFTEP%3E2.3.CO;2

Bunge, L., & Clarke, A. J. (2014). On the warm water volume and its changing relationship with ENSO. *Journal of Physical Oceanography*, *44*(5), 1372–1385. https://doi.org/10.1175/JPO-D-13-062.1

Cane, M. A. (1992). Tropical Pacific ENSO models: ENSO as a mode of the coupled system. In K. E. Trenberth (Ed.), *Climate System Modeling* (pp. 583–614). Cambridge University Press.

Cane, M. A., & Zebiak, S. E. (1985). A theory for El Niño and the Southern Oscillation. *Science*, *228*(4703), 1085–1087. https://doi.org/10.1126/science.228.4703.1085

Chang, P., Zhang, L., Saravanan, R., Vimont, D. J., Chiang, J. C. H., Ji, L., et al. (2007). Pacific meridional mode and El Niño—Southern Oscillation. *Geophysical Research Letters*, *34*(16), L16608. https://doi.org/10.1029/2007GL030302

Ding, R., Li, J., Tseng, Y., Sun, C., & Guo, Y. (2014). The Victoria mode in the North Pacific linking extratropical sea level pressure variations to ENSO. *Journal of Geophysical Research: Atmospheres*, *175*(4449), 27–45. https://doi.org/10.1038/175238c0

Ding, R., Li, J., Tseng, Y., Sun, C., & Xie, F. (2017). Joint impact of North and South Pacific extratropical atmospheric variability on the onset of ENSO events. *Journal of Geophysical Research: Atmospheres*, *122*(1), 279–298. https://doi.org/10.1002/2016JD025502

Ding, R., Tseng, Y.-H., Di Lorenzo, E., Shi, L., Li, J., Yu, J. Y., et al. (2022). Multi-year El Niño events tied to the North Pacific Oscillation. *Nature Communications*, *13*(1), 1–11. https://doi.org/10.1038/s41467-022-31516-9

Eyring, V., Bony, S., Meehl, G. A., Senior, C. A., Stevens, B., Stouffer, R. J., & Taylor, K. E. (2016). Overview of the Coupled Model Intercomparison Project Phase 6 (CMIP6) experimental design and organization [Dataset]. *Geoscientific Model Development*, *9*(5), 1937–1958. https://doi.org/10.5194/gmd-9-1937-2016

Fan, H., Huang, B., Yang, S., & Dong, W. (2021). Influence of the pacific meridional mode on ENSO evolution and predictability: Asymmetric modulation and ocean preconditioning. *Journal of Climate*, *34*(5), 1881–1901. https://doi.org/10.1175/JCLI-D-20-0109.1

Horii, T., Ueki, I., & Hanawa, K. (2012). Breakdown of ENSO predictors in the 2000s: Decadal changes of recharge/discharge-SST phase relation and atmospheric intraseasonal forcing. *Geophysical Research Letters*, *39*(10), L10707. https://doi.org/10.1029/2012GL051740

Hu, Z.-Z., Kumar, A., Huang, B., Zhu, J., L'Heureux, M., McPhaden, M. J., & Yu, J.-Y. (2020). The interdecadal shift of ENSO properties in 1999/2000: A review. *Journal of Climate*, *33*(11), 4441–4462. https://doi.org/10.1175/JCLI-D-19-0316.1

Hu, Z.-Z., Kumar, A., Ren, H.-L., Wang, H., L'Heureux, M., & Jin, F.-F. (2013). Weakened interannual variability in the tropical Pacific Ocean since 2000. *Journal of Climate*, *26*(8), 2601–2613. https://doi.org/10.1175/JCLI-D-12-00265.1

Hu, Z.-Z., Kumar, A., Zhu, J., Huang, B., Tseng, Y. H., & Wang, X. (2017). On the shortening of the lead time of ocean warm water volume to ENSO SST since 2000. *Scientific Reports*, *7*(1), 1–7. https://doi.org/10.1038/s41598-017-04566-z

Huang, P., & Xie, S.-P. (2015). Mechanisms of change in ENSO-induced tropical Pacific rainfall variability in a warming climate. *Nature Geoscience*, *8*(12), 922–926. https://doi.org/10.1038/ngeo2571

Jin, F.-F. (1997a). An equatorial ocean recharge paradigm for ENSO. Part I: Conceptual model. *Journal of the Atmospheric Sciences*, *54*(7), 811–829. https://doi.org/10.1175/1520-0469(1997)054<0811:AEORPF>2.0.CO;2

Jin, F.-F. (1997b). An equatorial ocean recharge paradigm for ENSO. Part II: A stripped-down coupled model. *Journal of the Atmospheric Sciences*, *54*(7), 830–847. https://doi.org/10.1175/1520-0469(1997)054<0830:AEORPF>2.0.CO;2

Kalnay, E., Kanamitsu, M., Kistler, R., Collins, W., Deaven, D., Gandin, L., et al. (1996). The NCEP/NCAR 40-Year Reanalysis Project [Dataset]. *Bulletin of the American Meteorological Society*, *77*(3), 437–471. https://doi.org/10.1175/1520-0477(1996)077<0437:TNYRP>2.0.CO;2

Kennedy, J. J. (2014). A review of uncertainty in in situ measurements and data sets of sea surface temperature. *Reviews of Geophysics*, *52*(1), 1–32. https://doi.org/10.1002/2013RG000434

Kumar, A., Chen, M., Xue, Y., & Behringer, D. (2015). An analysis of the temporal evolution of ENSO prediction skill in the context of the equatorial Pacific Ocean observing system. *Monthly Weather Review*, *143*(8), 3204–3213. https://doi.org/10.1175/MWR-D-15-0035.1

Larkin, N. K., & Harrison, D. E. (2005). Global seasonal temperature and precipitation anomalies during El Niño autumn and winter. *Geophysical Research Letters*, *32*(16), L16705. https://doi.org/10.1029/2005GL022860

Li, X., Hu, Z.-Z., & Becker, E. (2019). On the westward shift of tropical Pacific climate variability since 2000. *Climate Dynamics*, *53*(5–6), 2905–2918. https://doi.org/10.1007/s00382-019-04666-8

Lin, J. L. (2007). The double-ITCZ problem in IPCC AR4 coupled GCMs: Ocean-atmosphere feedback analysis. *Journal of Climate*, *20*(18), 4497–4525. https://doi.org/10.1175/JCLI4272.1

Liu, Z., & Alexander, M. (2007). Atmospheric bridge, oceanic tunnel, and global climatic teleconnections. *Reviews of Geophysics*, *45*(2), RG2005. https://doi.org/10.1029/2005RG000172

Lübbecke, J. F., & Mcphaden, M. J. (2014). Assessing the twenty-first-century shift in ENSO variability in terms of the Bjerknes stability index. *Journal of Climate*, *27*(7), 2577–2587. https://doi.org/10.1175/JCLI-D-13-00438.1

Martinez-Villalobos, C., Newman, M., Vimont, D. J., Penland, C., & David Neelin, J. (2019). Observed El Niño-La Niña asymmetry in a linear model. *Geophysical Research Letters*, *46*(16), 9909–9919. https://doi.org/10.1029/2019GL082922

McPhaden, M. J. (2012). A 21st century shift in the relationship between ENSO SST and warm water volume anomalies. *Geophysical Research Letters*, *39*(9), L09706. https://doi.org/10.1029/2012GL051826

Min, Q., Su, J., & Zhang, R. (2017). Impact of the south and north pacific meridional modes on the El Niño-Southern Oscillation: Observational analysis and comparison. *Journal of Climate*, *30*(5), 1705–1720. https://doi.org/10.1175/JCLI-D-16-0063.1

Plisnier, P. D., Serneels, S., & Lambin, E. F. (2000). Impact of ENSO on East African ecosystems: A multivariate analysis based on climate and remote sensing data. *Global Ecology and Biogeography*, *9*(6), 481–497. https://doi.org/10.1046/j.1365-2699.2000.00208.x

Rayner, N. A., Parker, D. E., Horton, E. B., Folland, C. K., Alexander, L. V., Rowell, D. P., et al. (2003). Global analyses of sea surface temperature, sea ice, and night marine air temperature since the late nineteenth century [Dataset]. *Journal of Geophysical Research*, *108*(D14), 4407. https://doi.org/10.1029/2002JD002670

Timmermann, A., An, S. I., Kug, J. S., Jin, F. F., Cai, W., Capotondi, A., et al. (2018). El Niño–Southern Oscillation complexity. *Nature*, *559*(7715), 535–545. https://doi.org/10.1038/s41586-018-0252-6

Vimont, D. J., Battisti, D. S., & Hirst, A. C. (2003). The seasonal footprinting mechanism in the CSIRO general circulation models. *Journal of Climate*, *16*(16), 2653–2667. https://doi.org/10.1175/1520-0442(2003)016<2653:TSFMIT>2.0.CO;2

Vimont, D. J., Wallace, J. M., & Battisti, D. S. (2003). The seasonal footprinting mechanism in the Pacific: Implications for ENSO. *Journal of Climate*, *16*(16), 2668–2675. https://doi.org/10.1175/1520-0442(2003)016<2668:TSFMIT>2.0.CO;2

Wang, W., Chen, M., & Kumar, A. (2010). An assessment of the CFS real-time seasonal forecasts. *Weather and Forecasting*, *25*(3), 950–969. https://doi.org/10.1175/2010WAF2222345.1

Wittenberg, A. T. (2009). Are historical records sufficient to constrain ENSO simulations? *Geophysical Research Letters*, *36*(12), L12702. https://doi.org/10.1029/2009GL038710

Xiang, B., Wang, B., & Li, T. (2013). A new paradigm for the predominance of standing central Pacific warming after the late 1990s. *Climate Dynamics*, *41*(2), 327–340. https://doi.org/10.1007/s00382-012-1427-8

Xie, P., & Arkin, P. A. (1997). Global precipitation: A 17-year monthly analysis based on gauge observations, satellite estimates, and numerical model outputs [Dataset]. *Bulletin of the American Meteorological Society*, *78*(11), 2539–2558. https://doi.org/10.1175/1520-0477(1997)078<2539:GPAYMA>2.0.CO;2

Xue, Y., Chen, M., Kumar, A., Hu, Z.-Z., & Wang, W. (2013). Prediction skill and bias of tropical Pacific sea surface temperatures in the NCEP Climate Forecast System version 2. *Journal of Climate*, *26*(15), 5358–5378. https://doi.org/10.1175/JCLI-D-12-00600.1

Yu, J.-Y., Kao, H.-Y., & Lee, T. (2010). Subtropics-related interannual sea surface temperature variability in the central equatorial Pacific. *Journal of Climate*, *23*(11), 2869–2884. https://doi.org/10.1175/2010JCLI3171.1

Yu, J.-Y., & Kim, S. T. (2011). Relationships between extratropical sea level pressure variations and the central Pacific and eastern Pacific types of ENSO. *Journal of Climate*, *24*(3), 708–720. https://doi.org/10.1175/2010JCLI3688.1

Zheng, F., Fang, X. H., Yu, J. Y., & Zhu, J. (2014). Asymmetry of the Bjerknes positive feedback between the two types of El Niño. *Geophysical Research Letters*, *41*(21), 7651–7657. https://doi.org/10.1002/2014GL062125

Zheng, F., Fang, X. H., Zhu, J., Yu, J. Y., & Li, X. C. (2016). Modulation of Bjerknes feedback on the decadal variations in ENSO predictability. *Geophysical Research Letters*, *43*(24), 12560–12568. https://doi.org/10.1002/2016GL071636